Polyhedron 117 (2016) 80–89

Contents lists available at ScienceDirect

Polyhedron

journal homepage: www.elsevier.com/locate/poly

Synthesis of new ferrocenyl dehydrozingerone derivatives and their effects on viability of PC12 cells

Sonia Pedotti [a], Angela Patti [a,*], Sonia Dedola [b], Antonio Barberis [c], Davide Fabbri [d], Maria Antonietta Dettori [d], Pier Andrea Serra [b,c], Giovanna Delogu [d,*]

[a] Istituto di Chimica Biomolecolare, CNR, Via Paolo Gaifami 18, 95126 Catania, Italy
[b] Dipartimento di Medicina Clinica e Sperimentale, Università di Sassari, Viale S. Pietro, 43/b, 07100 Sassari, Italy
[c] Istituto di Scienze Alimentari, CNR, Traversa la Crucca, 3, 07100 Sassari, Italy
[d] Istituto di Chimica Biomolecolare, CNR, Traversa la Crucca, 3, 07100 Sassari, Italy

ARTICLE INFO

Article history:
Received 13 April 2016
Accepted 15 May 2016
Available online 26 May 2016

Keywords:
Dehydrozingerone
Ferrocene
Hydroxylated biphenyls
PC12 cells
Oxidative stress

ABSTRACT

A series of novel compounds deriving from the conjugation of ferrocene with curcumin-related bioactive molecules as dehydrozingerone, zingerone and their biphenyl dimers was prepared by Claisen–Schmidt condensation of the suitable aromatic aldehydes and acetylferrocene in different conditions according to the starting material. The obtained compounds were fully characterized by NMR spectroscopy and cyclic voltammetry and reversible electrochemical behavior was recorded for monomer derivatives. The cell viability of PC12 cells after exposure to the organometallic compounds was also evaluated and a reduced toxicity with respect to the ferrocene was detected. In comparison with biphenyl **4**, a compound that manifested antiproliferative and apoptotic activities and was quite toxic on PC12 cells, the exposure to the ferrocenyl analogue **14** resulted in roughly fourfold increase in the cell viability. Ferrocenyl chalcones **14** and **16**–**18** significantly increased the oxidative stress generated by hydrogen peroxide, a molecule generally accumulated in cancer cells and, recently, studied as prodrug.

1. Introduction

Many efforts have been devoted to the development of new agents that, by targeting simultaneously multiple etiologies of a disease, may be more beneficial than selective agents for a single receptor site [1,2].

Curcumin **1** is a well-established active compound in dealing with different biochemical pathways leading to cancer. It is the major metabolite extracted from the rhizome of *Curcuma longa*, a plant routinely used in the preparation of curry spice as component of Asian traditional medicine (Fig. 1) [3,4].

A wide spectrum of biological properties (*e.g.* anti-inflammatory, anticancer, neuroprotective) attributed to curcumin has been related with its excellent free radical scavenging and antioxidant activities due to the presence of two guaiacyl moieties that proved to be very effective in stabilizing phenoxy radicals [5,6]. Unfortunately, curcumin has low solubility in aqueous and physiological solutions wherein it undergoes rapid degradation into ferulic acid, vanillin and dehydrozingerone **2** (Fig. 1) [7,8]. Like curcumin, dehydrozingerone **2** is known for its interesting anti-inflammatory and anticancer activities [9].

In a previous study we prepared compound **4**, the dimer of *O*Me-dehydrozingerone **3**, as the first curcumin-related biphenyl. We found that compound **4** was more active in inhibiting malignant melanoma and neuroblastoma cells growth when compared to curcumin itself (Fig. 1) [10]. Normal fibroblasts proliferation was not affected by this treatment therefore compound **4** could represent a good candidate in developing new therapies against neural crest-derived tumors.

Recently, we found that biphenyl **4** and biphenyl **5**, the latter being the biphenyl analogue of dehydrozingerone **2**, are able to partially inhibit the aggregation process of α-synuclein, suggesting the potential role of a hydroxylated biphenyl scaffold in the design of α-synuclein aggregation inhibitors in neurodegenerative pathologies [11]. Protective effects against oxidative stress induced in PC12 cells, a neuronal cell model, was also investigated for biphenyls **4** and **5** and their derivatives.

Compared to phenols, hydroxylated biphenyls display higher antioxidant activity in virtue of the presence of two hydroxyl groups at the *ortho–ortho′* positions generally providing reduction in toxicity compared with the corresponding phenolic monomer [12,13].

* Corresponding authors. Tel.: +39 0957 338328 (A. Patti). Tel.: +39 0792841220 (G. Delogu).
E-mail addresses: angela.patti@icb.cnr.it (A. Patti), giovanna.delogu@ss.icb.cnr.it (G. Delogu).

http://dx.doi.org/10.1016/j.poly.2016.05.039
0277-5387/

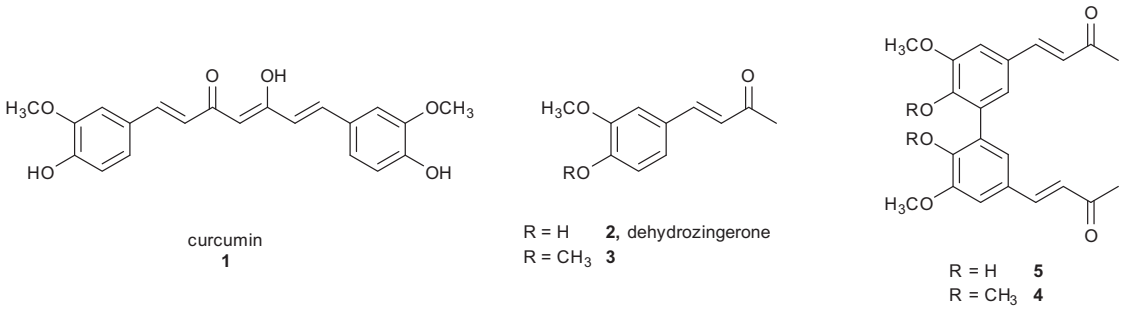

Fig. 1. Natural and natural-like phenols and biphenols.

Ferrocene is a neutral, chemically stable, relatively non toxic molecule whose good reversible redox proprieties seem to be strongly associated with the biological activity. As an example, the activity of tamoxifen, the most common drug used to treat patients diagnosed with breast cancer, was enhanced when a unit of ferrocene is covalently bonded to the molecule of hydroxytamoxifen, the active metabolite and it was thought that the extended π-system in hydroxytamoxifen-ferrocene conjugate plays an important role in the mode of action of the drug [14,15].

The organometallic approach has been successfully applied to other bioactive compounds like flavones [16], amino acids [17,18], chalcones [19,20], quinolinones [21], ellagitannins [22], cyclodextrin [23] and curcumin [24,25]. Although several ferrocenyl-curcumin derivatives were prepared by different groups, all of them contain a β-diketoeptadiene or pentenedienone chain in their structure [24,25].

Ferrocene derivatives of dehydrozingerone, zingerone and the corresponding C_2-symmetric dimers have not been synthetized so far and here we report their preparation and characterization. The electrochemical properties and cytotoxic activity in PC12 cells of the obtained compounds was also evaluated in comparison with data of the corresponding compounds lacking in ferrocene unit.

2. Experimental section

2.1. Instrumentation

^{1}H and ^{13}C NMR spectra were registered in $CDCl_3$ at 400.13 and 100.69 MHz respectively on a Bruker Avance™ 400 instrument. 2D-NMR experiments were performed using standard Bruker microprograms. All NMR spectra were recorded using $CDCl_3$ unless otherwise specified. Chemical shifts (δ) are given as ppm relative to the residual solvent peak and coupling constants (J) are in Hz. In the NMR assignments, Cp and Cp′ refer to substituted and unsubstituted cyclopentadienyl rings, respectively. UV spectra were recorded with a spectrometer Perkin-Elmer Lambda 35 in dichloromethane at concentration of 0.74×10^{-5} M. Elemental analyses were obtained from the Department of Pharmaceutical Sciences, University of Catania. Melting points are uncorrected. Cyclic voltammetries were performed with an eDAQ QuadStat, an e-Corder 410 and the Echem software (eDAQ Europe, Poland).

2.2. Materials

Sodium hydroxide microprills were purchased from Riedel-de-Haën (Germany). Column chromatography was performed on Si 60 (230–400 mesh) silica gel using the specified eluants. Ferrocene, veratraldehyde, hydrogen peroxide were purchased from Sigma–Aldrich (Milan, Italy), vanillin from Alfa Aesar GmbH & Co KG (Karlsruhe, Germany) and zingerone from Chemos GmbH (Regenstanf, Germany). All solvents of purity >98% (GC) were used as received.

2.3. General procedure for the O-benzylation of vanillin and divanillin

To a solution of the suitable aldehyde (1 mmol) in DMF (5 mL), K_2CO_3 (2 eqv.) and 4-methylbenzylbromide (1.1 eqv.) were added and the suspension stirred at room temperature until complete conversion of the substrate was detected by TLC analysis (12–20 h). The solvent was then evaporated *in vacuo* and the residue dissolved in AcOEt (15 mL) and treated with satd. NH_4Cl solution (3×10 mL). The organic phase, extracted, then was washed with brine, dried over Na_2SO_4 and taken to dryness to give a residue that was purified by chromatographic column (*n*-hexane:AcOEt 9:1) to give pure *O*-(4-methyl)benzyl derivatives.

2.3.1. 3-Methoxy-4-(4-methyl)benzyloxy-benzaldehyde (**9**)

95% yield, white solid, mp = 69–71 °C; ^{1}H NMR: δ 2.36 (s, 3H, Me), 3.94 (s, 3H, OMe), 5.21 (s, 2H, CH_2), 6.99 (d, 1H, J = 8.0, H-5), 7.20 (d, 2H, J = 8.0, ArH), 7.33 (d, 2H, J = 8.0, ArH), 7.39 (dd, 1H, J = 1.6 and 8.0, H-6), 7.43 (d, 1H, J = 1.6, H-3), 9.84 (s, 1H, CHO); ^{13}C NMR: δ 21.1 (Me), 55.9 (OMe), 70.7 (CH_2), 109.2 (ArH), 112.3 (ArH), 126.5 (ArH), 127.2 (2× ArH), 129.3 (2× ArH), 130.1 (Ar), 132.8 (Ar), 137.9 (Ar), 150.0 (Ar), 153.6 (Ar), 190.8 (CHO). *Anal.* Calc. for $C_{16}H_{16}O_3$: C, 74.97; H, 6.30. Found: C, 75.05; H, 6.28%.

2.3.2. 2,2′-Di(4-methyl)benzyloxy-3,3′-dimethoxy-5,5′-diformyl-1,1′-biphenyl (**13**)

93% yield, white solid, mp = 128–129 °C; ^{1}H NMR: δ 2.27 (s, 6H, Me), 4.00 (s, 6H, OMe), 4.89 (s, 4H, CH_2), 6.88 (d, 4H, J = 8.0, ArH), 6.96 (d, 4H, J = 8.0, ArH), 7.14 (d, 2H, J = 1.6, H-6 and H-6′), 7.49 (d, 2H, J = 1.6, H-4 and H-4′), 9.77 (s, 2H, CHO); ^{13}C NMR: δ 21.0 (Me), 56.0 (OMe), 74.5 (CH_2), 109.6 (Ar-H), 128.1 (ArH), 128.2 (2× ArH), 128.7 (2× ArH), 131.7 (Ar), 132.4 (Ar), 133.7 (Ar), 137.6 (Ar), 150.0 (Ar), 153.4 (Ar), 191.0 (CHO). *Anal.* Calc. for $C_{32}H_{30}O_6$: C, 75.26; H, 5.93. Found: C, 75.32; H, 5.90%.

2.4. Solvent-free procedure for the synthesis of ferrocenyl chalcones (Method A)

A 10-mL sealed vial charged with the suitable *O*-protected aldehyde (0.5 mmol) and acetylferrocene (0.5 mmol) was placed in a bath oil at 100 °C and solid NaOH (1.0 mmol) was added. The mixture was stirred vigorously and left to react until the TLC analysis showed complete disappearance of substrates (1–3 h). After addition of CH_2Cl_2 (10 mL) the mixture was partitioned with satd. NH_4Cl solution (3×5 mL) and the organic layer, extracted, was washed with brine and dried over Na_2SO_4. The organic solvent was then removed *in vacuo* and the residue recrystallized from *n*-hexane/CH_2Cl_2 to give pure chalcones.

*2.4.1. 1-Ferrocenyl-3-(3,4-dimethoxy)phenyl-2-propen-1-one (**10**)*

68% yield, red solid, mp = 155–156 °C; ^{1}H NMR: δ 3.94 (s, 3H, OMe), 3.97 (s, 3H, OMe), 4.22 (s, 5H, Cp′), 4.58 (bs, 2H, Cp), 4.93 (bs, 2H, Cp), 6.92 (d, 1H, *J* = 8.4, ArH), 7.00 (d, 1H, *J* = 15.6, H-2), 7.15 (s, 1H, ArH), 7.26 (d, 1H, *J* = 8.4, ArH), 7.75 (d, 1H, *J* = 15.6, H-3); ^{13}C NMR: δ 55.9 (OMe), 69.6 (CpH), 70.0 (Cp′H), 72.5 (CpH), 80.6 (Cp), 110.4 (ArH), 111.1 (ArH), 120.9 (C-2), 122.3 (ArH), 128.0 (Ar), 140.9 (C-3), 149.1 (Ar), 151.0 (Ar), 192.8 (CO). *Anal.* Calc. for $C_{21}H_{20}FeO_3$: C, 67.02; H, 5.36. Found: C, 66.98; H, 5.38%.

*2.4.2. 1-Ferrocenyl-3-[3-methoxy-4-(4-methylbenzyloxy)]phenyl-2-propen-1-one (**11**)*

75% yield, red solid, mp = 149–150 °C; ^{1}H NMR: δ 2.36 (s, 3H, Me), 3.97 (s, 3H, OMe), 4.21 (s, 5H, Cp′), 4.58 (t, 2H, *J* = 1.6, Cp), 4.91 (t, 2H, *J* = 1.6, Cp), 5.19 (s, 2H, CH_2), 6.92 (d, 1H, *J* = 8.4, ArH), 6.99 (d, 1H, *J* = 15.6, H-2), 7.18 (m, 4H, ArH), 7.34 (d, 2H, *J* = 8.0, ArH), 7.74 (d, 1H, *J* = 15.6, H-3); ^{13}C NMR: δ 21.1 (Me), 56.1 (OMe), 69.6 (CpH), 70.0 (Cp′H), 70.8 (CH_2), 72.5 (CpH), 80.7 (Cp), 111.1 (ArH), 113.5 (ArH), 120.9 (C-2), 122.1 (ArH), 127.2 (2× ArH), 128.3 (Ar), 129.2 (2× ArH), 133.5 (Ar), 137.7 (Ar), 140.9 (C-3), 149.7 (Ar), 150.2 (Ar), 192.8 (CO). *Anal.* Calc. for $C_{28}H_{26}FeO_3$: C, 72.10; H, 5.62. Found: C, 72.19; H, 5.64%.

2.5. Synthesis of ferrocenyl chalcones in solution (Method B)

To a solution of the suitable *O*-protected dialdehyde (0.5 mmol) and acetylferrocene (1.0 mmol) in dioxane (10 mL) NaOH (2.0 mmol) was added and the mixture stirred at 40 °C for 48–96 h. The solution was concentrated by evaporation of the solvent and partitioned between CH_2Cl_2 (10 mL) and satd. NH_4Cl solution (3 × 5 mL). The organic layer washed with brine, dried over Na_2SO_4 and taken to dryness to give a residue that was purified on Si gel column (*n*-hexane:AcOEt:CH_2Cl_2 3:1:1).

*2.5.1. (2E,2′E)-3,3′-(1,1′-Biphenyl-5,5′,6,6′-tetramethoxy-3,3′-diyl)bis (1-ferrocenyl-2-propen-1-one), (**14**)*

38% yield, red solid, mp = 185–186 °C; ^{1}H NMR: δ 3.77 (s, 6H, OMe), 4.02 (s, 6H, OMe), 4.22 (s, 10H, Cp′), 4.59 (br s, 4H, Cp), 4.92 (br s, 4H, Cp), 7.05 (d, 2H, *J* = 15.6, 2× H-2), 7.21 (br s, 2H, ArH), 7.27 (br s, 2H, ArH), 7.79 (d, 2H, *J* = 15.6, 2× H-3); ^{13}C NMR: δ 56.0 (OMe), 60.8 (OMe), 69.7 (CpH), 70.0 (Cp′H), 72.6 (CpH), 80.5 (Cp), 112.1 (ArH), 122.2 (C-2), 122.9 (ArH), 130.6 (Ar), 132.5 (Ar), 140.5 (C-3), 148.6 (Ar), 152.9 (Ar), 192.8 (CO). *Anal.* Calc. for $C_{42}H_{38}Fe_2O_6$: C, 67.20; H, 5.11. Found: C, 67.27; H, 5.12%.

*2.5.2. (2E,2′E)-3,3′-[1,1′-Biphenyl-5,5′-dimethoxy-6,6′-di(4-methyl) benzyloxy-3,3′-diyl]bis(1-ferrocenyl-2-propen-1-one), (**15**)*

90% yield, red solid, mp = 183–185 °C; ^{1}H NMR: δ 2.24 (s, 6H, Me), 3.98 (s, 6H, OMe), 4.19 (s, 10H, Cp′), 4.57 (br s, 4H, Cp), 4.83 (s, 4H, CH_2), 4.89 (br s, 4H, Cp), 6.98 (s, 8H, ArH), 7.00 (d, 2H, *J* = 15.6, 2× H-2), 7.20 (br s, 2H, ArH), 7.29 (br s, 2H, ArH), 7.77 (d, 2H, *J* = 15.6, 2× H-3); ^{13}C NMR: δ 21.1 (Me), 56.1 (OMe), 69.7 (CpH), 70.0 (Cp′H), 72.6 (CpH), 74.5 (CH_2), 80.5 (Cp), 112.4 (ArH), 122.1 (C-2), 123.1 (ArH), 128.1 (4× ArH), 128.7 (4× ArH) 130.5 (Ar), 132.9 (Ar), 134.1 (Ar), 137.4 (Ar), 140.6 (C-3), 147.5 (Ar), 153.2 (Ar), 192.8 (CO). *Anal.* Calc. for $C_{56}H_{50}Fe_2O_6$: C, 72.25; H, 5.42. Found: C, 72.35; H, 5.40%.

*2.6. 1-Ferrocenyl-3-(3-methoxy-4-hydroxy)phenyl-propan-1-one (**16**)*

A solution of compound **11** (100 mg, 0.21 mmol) in THF (5 mL) was placed in a 100 mL flask equipped with a Teflon stopcock and Pd/C carbon (10% Pd on activated carbon, 10 mg) was added. After the flask was evacuated and then refilled with H_2 (1.0 atm), the reaction mixture was stirred at 60 °C for 3 h. The suspension was then filtered through a short plug of Celite and the solution evaporated. The residue was purified by column chromatography (*n*-hexane:AcOEt 4:1) to give pure **16** (62 mg, 0.17 mmol, 81% yield) as an orange solid, mp = 133–134 °C; ^{1}H NMR: δ 2.99 (m, 4H, CH_2), 3.90 (s, 3H, OMe), 4.11 (s, 5H, Cp′), 4.49 (t, 2H, *J* = 1.6, Cp), 4.77 (t, 2H, *J* = 1.6, Cp), 5.54 (s, 1H, OH), 6.78 (dd, 1H, *J* = 1.6 and 8.0, ArH-6), 6.80 (d, 1H, *J* = 1.6, ArH-2), 6.87 (d, 1H, *J* = 8.0, ArH-5); ^{13}C NMR: δ 29.8 (C-3), 41.8 (C-2), 55.9 (OMe), 69.2 (CpH), 69.6 (Cp′H), 72.1 (CpH), 78.9 (Cp), 111.3 (ArH), 114.3 (ArH), 120.9 (ArH), 133.4 (Ar), 143.9 (Ar), 146.3 (Ar), 203.3 (CO). *Anal.* Calc. for $C_{20}H_{20}FeO_3$: C, 65.94; H, 5.54. Found: C, 65.89; H, 5.52%.

*2.7. 3,3′-(5,5′-Dimethoxy,6,6′-dihydroxy-[1,1′-biphenyl]-3,3′-diyl)bis (1-ferrocenyl-propan-1-one), (**17**)*

According the same procedure described above, *O*-benzyl derivative **15** (102 mg, 0.11 mmol) was hydrogenated to give compound **17**, obtained as an orange solid (65 mg, 0.09 mmol, 82% yield) after purification on Si gel column (*n*-hexane:AcOEt:CH_2Cl_2 4:3:3), mp = 93–94 °C; ^{1}H NMR (CD_3COCD_3): δ 2.96 (br t, 4H, CH_2), 3.06 (br t, 4H, CH_2), 3.88 (s, 6H, OMe), 4.13 (s, 10H, Cp′), 4.50 (s, 4H, Cp), 4.80 (s, 4H, Cp), 6.85 (s, 2H, ArH), 6.95 (s, 2H, ArH); ^{13}C NMR (CD_3COCD_3): δ 29.4 (CH_2), 41.4 (CH_2), 55.5 (OMe), 69.1 (CpH), 69.4 (Cp′H), 71.7 (CpH), 79.4 (Cp), 111.3 (ArH), 123.3 (ArH), 125.3 (Ar), 132.7 (Ar), 141.7 (Ar), 147.8 (Ar), 202.0 (CO). *Anal.* Calc. for $C_{40}H_{38}Fe_2O_6$: C, 66.12; H, 5.28. Found: C, 66.22; H, 5.26%.

*2.8. 1-Ferrocenyl-3-(3-methoxy-4-hydroxy)phenyl-2-propen-1-one, (**18**)*

To a solution of **11** (100 mg, 0.21 mmol) in dry CH_2Cl_2 (5 mL) was added $(CH_3)_3SiI$ (0.24 mmol, 33 μL) and the mixture left to react at room temperature for 3 h. The reaction mixture was then quenched with satd. $NaHCO_3$ (3 × 5 mL). The organic phase was extracted and washed with brine and finally taken to dryness. The residue was purified by chromatographic column (*n*-hexane: AcOEt 4:1) to give **18** (0.18 mmol, 64 mg, 84% yield) as a deep red solid, mp = 138–139 °C; ^{1}H NMR: δ 3.99 (s, 3H, OMe), 4.22 (s, 5H, Cp′), 4.59 (t, 2H, *J* = 2.0, Cp), 4.93 (t, 2H, *J* = 2.0, Cp), 6.01 (s, 1H, OH), 6.90 (d, 1H, *J* = 15.6, H-2), 7.00 (d, 1H, *J* = 7.6, ArH), 7.11 (d, 1H, *J* = 1.6, ArH), 7.26 (dd, 1H, *J* = 1.6 and 7.6, ArH), 7.75 (d, 1H, *J* = 15.6, H-3); ^{13}C NMR: δ 55.9 (OMe), 69.6 (CpH), 70.0 (Cp′H), 72.5 (CpH), 80.6 (Cp), 110.4 (ArH), 114.8 (ArH), 120.6 (C-2), 122.4 (ArH), 127.6 (Ar), 141.1 (C-3), 146.7 (Ar), 147.8 (Ar), 192.9 (CO); *Anal.* Calc. for $C_{20}H_{18}FeO_3$: C, 66.30; H, 5.01. Found: C, 66.21; H, 4.99%.

*2.9. (2E,2′E)-3,3′-[1,1′-biphenyl-5,5′-dimethoxy-6,6′-dihydroxy-3,3′-diyl]bis(1-ferrocenyl-2-propen-1-one) (**19**)*

According the procedure described above, compound **15** (102 mg, 0.11 mmol) was deprotected at the benzyl group to afford compound **19** as a dark red solid (28 mg, 0.04 mmol, 36% yield) after purification by chromatographic column (*n*-hexane:AcOEt: CH_2Cl_2 4:3:3), mp = 139–140 °C; ^{1}H NMR: δ 4.06 (s, 6H, OMe), 4.22 (s, 10H, Cp′), 4.58 (br s, 4H, Cp), 4.93 (br s, 4H, Cp), 6.25 (br s, 2H, OH), 7.04 (d, 2H, *J* = 15.6, H-2), 7.19 (s, 2H, ArH), 7.37 (s, 2H, ArH), 7.80 (d, 2H, *J* = 15.6, H-3); ^{13}C NMR: δ 56.2 (OMe), 69.7 (CpH), 70.0 (Cp′H), 72.6 (CpH), 80.4 (Cp), 110.4 (ArH), 121.4 (C-2), 123.6 (ArH), 123.9 (Ar), 127.4 (Ar), 141.1 (C-3), 145.1 (Ar), 147.2 (Ar), 192.8 (CO); *Anal.* Calc. for $C_{40}H_{34}Fe_2O_6$: C, 66.49; H, 4.75. Found: C, 66.58; H, 4.76%.

2.10. Electrochemical measurements

The electrochemical behavior of compounds **2**–**4**, **6**–**7** and the corresponding ferrocenyl derivatives **10**, **14**, **16**, **17** and **18** was evaluated by cyclic voltammetry (CV) in a buffer solution containing 10 mL of KNO_3 1 M and 10 mL of ethanol 96%, using a carbon working electrode (area 0.071 mm^2), an Ag/AgCl reference electrode and a Pt counter electrode, with a scanned potential range (Vapp) comprised between −1000 mV and +1000 mV, at 100 mV s^{-1} scan rate, in the absence and in the presence of 1 mM of each compound.

2.11. Cell culture and treatments

PC12 cells were grown in Dulbecco's modified Eagle's medium: Nutrient Mixture F-12 (DMEM-F12) containing 10% horse serum, 5% fetal bovine serum (FBS) and 1% penicillin (5000 U/mL)/streptomycin (5000 μg/mL) at 37 °C under humidified 5% CO_2/air. Stock H_2O_2 (5 mM) solution was prepared in Milli-Q water and diluted (20–100 μM) in complete medium. Ferrocene and compounds **10**, **14**, **16**, **17**, **18** solutions (100 mM) were prepared in DMSO and then diluted to the final concentration in complete medium, containing a concentration of DMSO <0.1%. All solutions were prepared immediately before use. All experiments were performed on PC12 cells during their exponential phase of growth. In a separate series of experiments the cells have been exposed to ferrocene alone (40 μM). In a previous experiment [11], we determined at 40 μM the protective concentration of compounds **2**–**7**, against the cell death induced by H_2O_2; this concentration was used in all experiments with the corresponding compounds with ferrocenyl unit, done in triplicate.

2.12. MTT assay

For each experiment, 1×10^5 PC12 cells/cm^2 were plated and treated 24 h later (time 0). PC12 cells were preincubated for 20 min with ferrocene or ferrocenyl chalcones and then exposed to H_2O_2 (75 μM) for 24 h; at this concentration, H_2O_2 alone determined a cell death around 40%. PC12 cell viability was evaluated using the 3,(4,5-dimethylthiazol-2-yl)2,5-diphenyltetrazoliumbromide (MTT) reduction assay [26]. The metabolic dye MTT is reduced by viable cells to form blue formazan crystals. In brief, the cells were incubated with 1 mg of MTT per milliliter of medium, and the cultures were allowed to incubate at 37 °C for 4 h. The MTT was removed, and the cells were rinsed with PBS and centrifuged at 4000 rpm for 15 min. Thereafter, the supernatant was discarded, and the pellet was dissolved in 2 mL of isopropanol; after centrifugation at 4000 rpm for 5 min, the color was read at 578 nm using a Bauty Diagnostic microplate reader. Experiments were done in triplicate. A standard curve was constructed with different concentrations of cells at the start of every experiment.

3. Results and discussion

3.1. Synthesis

Dehydrozingerone **2** was chosen as reference structure and, in order to preserve the guaiacyl unit present in the molecule and to extend the π-delocalization, the electroactive ferrocenyl moiety was inserted at the end of the unsaturated chain in place of the methyl group. One and two ferrocenyl units were introduced in dehydrozingerone derivatives **3**, **4** and **5**, respectively. The study was also extended to the preparation of ferrocenyl conjugates of zingerone **6**, the non-volatile component of *Zingiber officinale* [27], and its C_2-symmetric dimer **7** in view of the known influence of butan-2-one chain in the antioxidant and anti-inflammatory activities of **6** (Scheme 1) [28–30].

Monomers **2**, **3** and dimers **4**, **5** were prepared from vanillin as previously described by us [10a], whereas dimer **7** was prepared from zingerone **6**, commercially available [11].

For the synthesis of the target ferrocenyl chalcones, a Claisen–Schmidt condensation of acetylferrocene and the suitable *O*-protected vanillin was carried out in solvent-free conditions (Method A) according to a previously reported procedure by us that generally provides short reaction times (Scheme 2) [31]. By this route, ferrocenyl chalcone **10**, the organometallic analogue of **3**, was obtained in 68% isolated yield starting from *O*Me-vanillin **8**.

However, when *O*Me-divanillin **12** was used as substrate, the conventional reaction in solution was preferred (Method B) because it gave better yields of the desired ferrocenyl derivative with only negligible amounts of the intermediate product deriving from a single Claisen–Schmidt condensation (Scheme 3). Starting from *O*Me-divanillin and acetylferrocene compound **14**, the ferrocenyl analogue of biphenyl **4**, was obtained in moderate yield.

Reactions of acetylferrocene with vanillin or divanillin was not effective to obtain derivatives bearing free hydroxyl groups. When the starting aldehydes were converted into the corresponding *O*-benzylethers **9** and **13** and then subjected to Claisen–Schmidt condensation, the corresponding ferrocenyl chalcones **11** and **15** were achieved in 75% and 90% yields, respectively (Method A for compound **9** and Method B for compound **13** in the Experimental section).

Hydrogenation of **11** and **15** in the presence of Pd/charcoal catalyst allowed the simultaneous reduction of the ethylenic bond and deprotection of *O*-benzyl ether affording the zingerone-like derivative **16** and the corresponding dimer **17**, respectively (Scheme 4). Selective deprotection at room temperature of *O*-benzyloxygroups in **11** or **15** with Me_3SiI was exploited for the preparation of **18** and **19** in which the ethylenic bonds were retained (Scheme 4). However, dimeric compound **19**, was rather unstable and for this reason it was not further investigated.

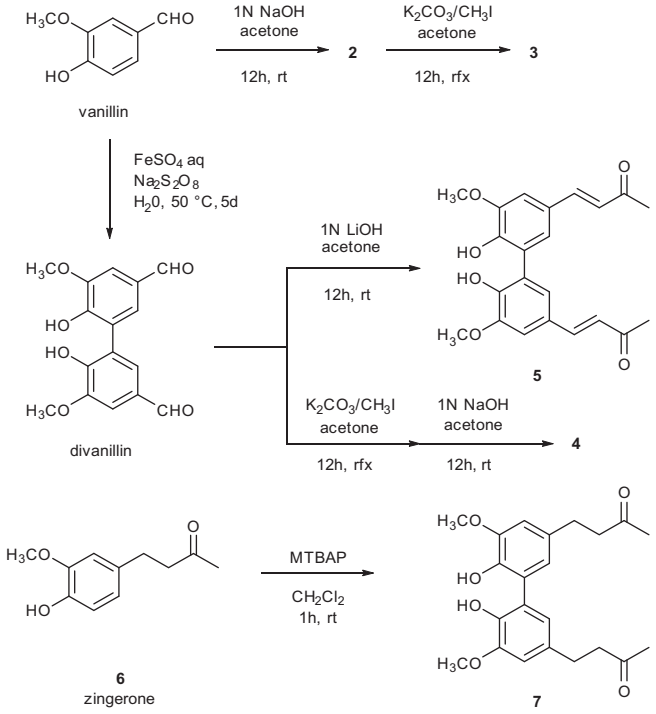

Scheme 1. Synthesis of benzalacetones **2**–**5** and **7**.

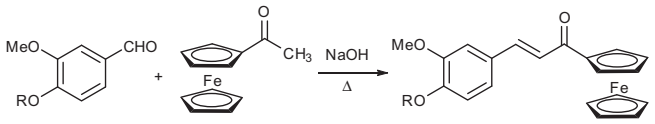

8 R = Me
9 R = (4-Me)Bn

10 R = Me
11 R = (4-Me)Bn

Scheme 2. Synthesis of ferrocenyl chalcones **10** and **11**.

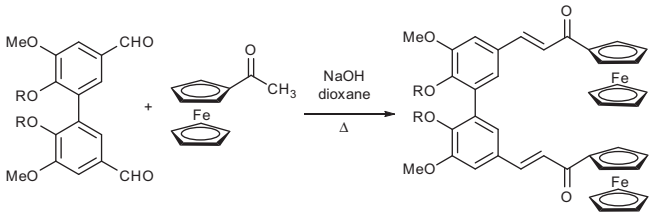

12 R = Me
13 R = (4-Me)Bn

14 R = Me
15 R = (4-Me)Bn

Scheme 3. Synthesis of ferrocenyl chalcones **14** and **15**.

Exclusive formation of *trans*-isomers of ferrocenyl chalcones was deduced from their ^{1}H NMR spectra in solution that displayed a large coupling constant (J = 15.6 Hz) for the doublets of the ethylenic protons. Concerning the ferrocenyl unit, the NMR spectra of dimers appeared quite similar to those of monomeric counterparts, this spectroscopic evidence should exclude any interaction with the two metallocene units when both present in the same molecular structure. Downfield shifts of about 10 ppm were observed for ^{13}C NMR carbonyl resonances going from enone-containing derivatives to the corresponding saturated compounds.

UV–Vis absorption spectra of ferrocenyl chalcones **18**, **10** and **14** recorded in dichloromethane at concentration 0.74 × 10^{-5} M tend to have larger conjugated systems compared to their corresponding chalcones **2**, **3**, **4** (Supplementary data), and therefore their peak wavelengths tend to be shifted toward the long wavelength region.

3.2. Voltammetric measurements

All the prepared ferrocenyl derivatives were subjected to cyclic voltammetric analysis and also the parent benzalacetones were included in the study for comparative purposes. According to Wang et al. [32], the reversibility of electrochemical processes of each compound, was evaluated by comparing the magnitude of the separation between the oxidation (E_{ox}) and reduction (E_{red}) peak potentials, $\Delta E_p = |E_{ox} - E_{red}|$, with the corresponding value of the reversible system ferrocene/ferricenium couple.

Cyclic voltammograms are showed in Figs. 2–6 and E_{ox}, E_{red} and ΔE_p of all compounds are listed in Table 1.

Dehydrozingerone **2** and zingerone **6** displayed not reversible behavior and compound **3**, lacking in free phenolic-OH group, was electrochemically inert.

On the contrary, cyclovoltammetric spectra of the corresponding monomeric ferrocenyl analogues, e. g. **10**, **16** and **18**, showed a reversible one-electron redox couple attributed to the ferrocenyl unit bonded to the aliphatic chain whereas the ΔE_p value was influenced by the molecule structure.

In the dimer series, no significant electrochemical response was detected for **4** and **14** (Fig. 4) while compounds **7** and **17**, the zingerone dimer and its ferrocenyl analogue, showed not reversible electrochemical behavior probably due to the *ortho–ortho′* free phenolic-OH groups that can activate side reactions as described in literature for other biphenyls with similar structural features (Fig. 6) [33,34].

A putative interaction between the two ferrocenyl units in dimer **17,** favoured by the phenolic –OH hydrogen bond and resulting in forcing closer the aliphatic side chains could not be ruled out. On the contrary, the lack of hydrogen bond in dimer **14** would drive the biphenyl structure in a conformation where the two ferrocenyl units are each other far away.

For all ferrocenyl derivatives a drastic shift to positive peak potentials was observed with respect to ferrocene probably due to the electron-withdrawing properties of the rest of the molecule as observed in other ferrocenyl conjugates [35]. A broad oxidation peak at low potential was observed for compounds **10**, **16**, **17** and **18** (Figs. 2–6) probably due to an oxidation process which involves the organic part of the molecule before that the Fe oxidation process takes place [36,37]. The presence of an unsaturated bond in the side chain produced a drastic decrease in the potential value detected for dehydrozingerone **2** compared to zingerone **6** (E_{ox} 250 mV versus E_{ox} 422 mV). Nevertheless, when a ferrocenyl unit is embedded in a saturated chain as in **16** and dimer **17** the E_{ox}/E_{red} value shifted to lower potentials compared to the parent compound lacking in the electroactive unit (eg. **6** and **7**). It seems that both iron atom in ferrocene and phenolic hydroxyl group played a

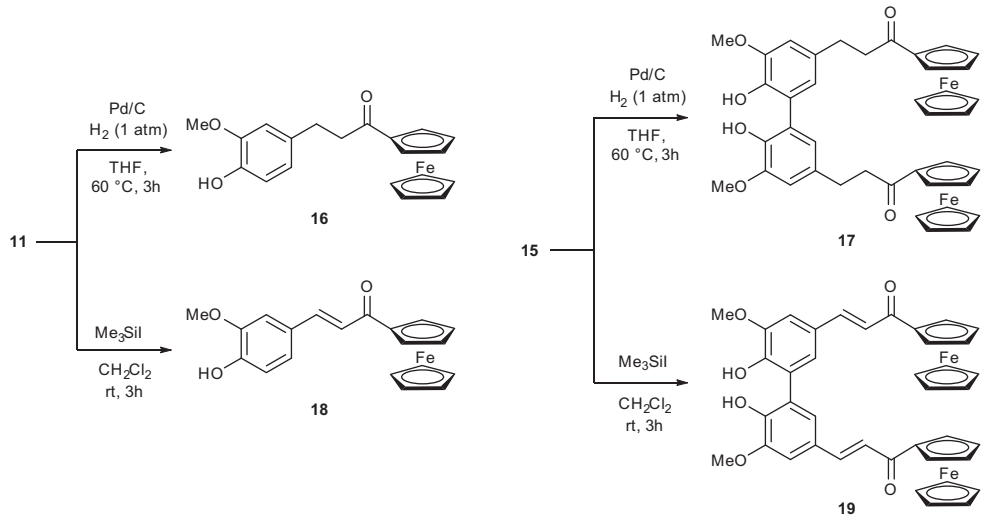

Scheme 4. Synthesis of ferrocenyl chalcones **16**–**19**.

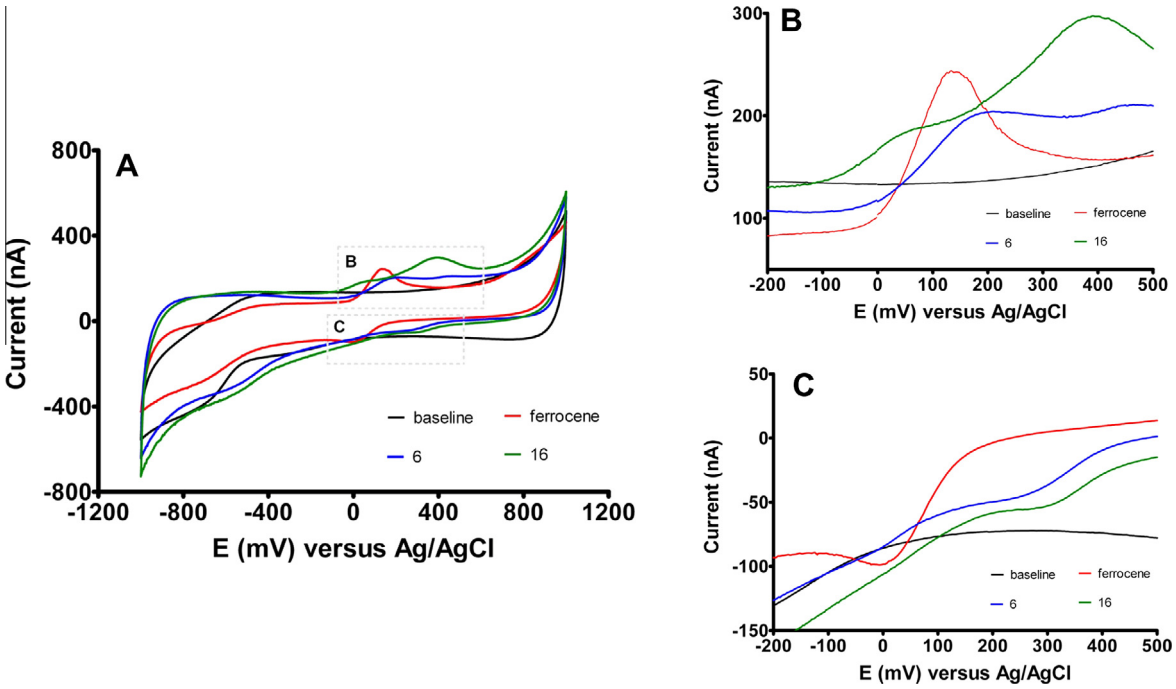

Fig. 2. Cyclic voltammograms recorded with a carbon working electrode (area = 0.071 cm^2), in a buffer solution containing 10 mL of KNO_3 1 M and 10 mL of ethanol 96%. Curves in A, obtained with a scanned potential range (E_{app}) comprised between −1000 mV and +1000 mV, at 100 mV s^{-1} scan rate, were separately achieved, in the absence and in the presence of 1 mM ferrocene, 1 mM compound **6** and 1 mM compound **16**; curves in B are details of voltammogram A, in a scanned potential range (E_{app}) comprised between −200 mV and +500 mV, where oxidation peak of each compound is enhanced; curves in C are details of voltammogram A, in a scanned potential range (E_{app}) comprised between −200 mV and +500 mV, where reduction peak of each compound is enhanced.

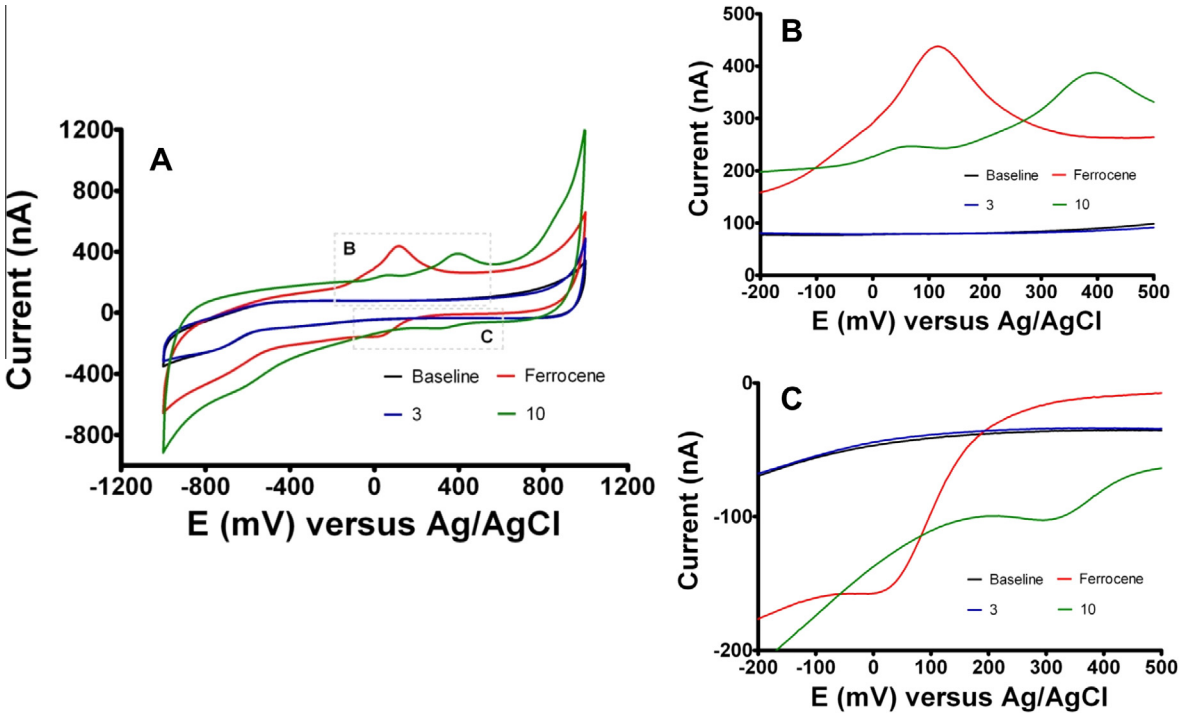

Fig. 3. Cyclic voltammograms recorded with a carbon working electrode (area = 0.071 cm^2), in a buffer solution containing 10 mL of KNO_3 1 M and 10 mL of ethanol 96%. Curves in A, obtained with a scanned potential range (E_{app}) comprised between −1000 mV and +1000 mV, at 100 mV s^{-1} scan rate, were separately achieved, in the absence and in the presence of 1 mM ferrocene, 1 mM compound **3** and 1 mM compound **10**; curves in B are details of voltammogram A, in a scanned potential range (E_{app}) comprised between −200 mV and +500 mV, where oxidation peak of each compound is enhanced; curves in C are details of voltammogram A, in a scanned potential range (E_{app}) comprised between −200 mV and +500 mV, where reduction peak of each compound is enhanced.

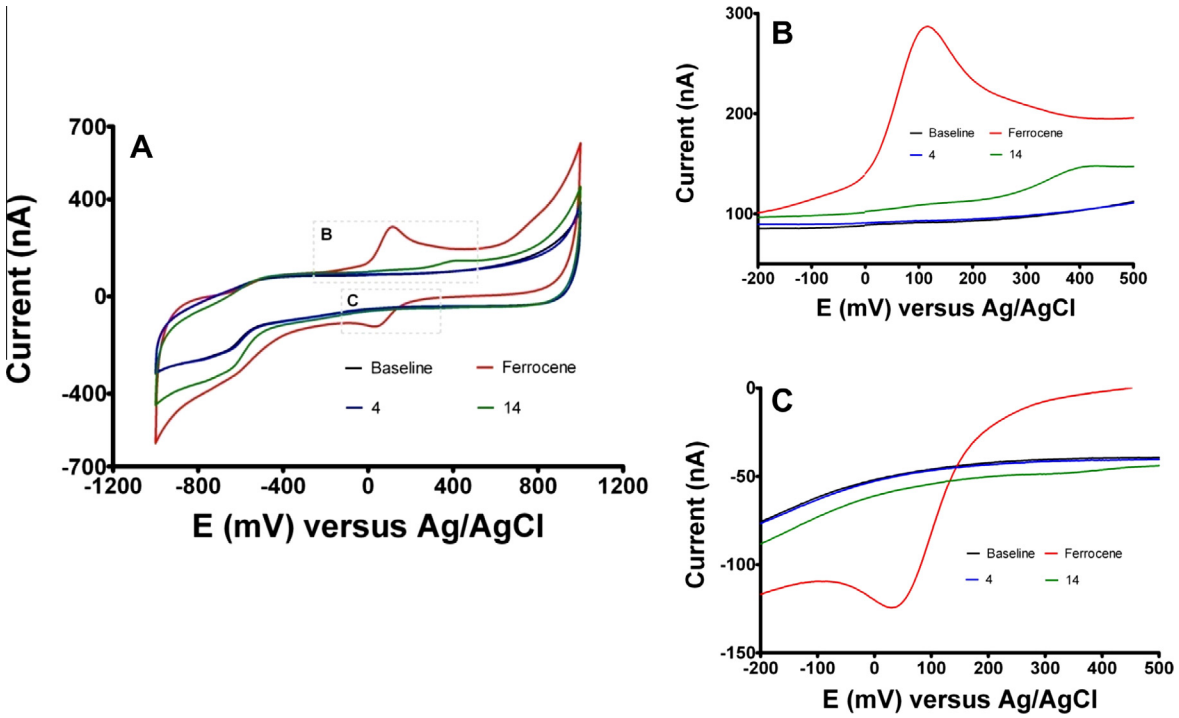

Fig. 4. Cyclic voltammograms recorded with a carbon working electrode (area = 0.071 cm^2), in a buffer solution containing 10 mL of KNO_3 1 M and 10 mL of ethanol 96%. Curves in A, obtained with a scanned potential range (E_{app}) comprised between −1000 mV and +1000 mV, at 100 mV s^{-1} scan rate, were separately achieved, in the absence and in the presence of 1 mM ferrocene, 1 mM compound **4** and 1 mM compound **14**; curves in B are details of voltammogram A, in a scanned potential range (E_{app}) comprised between −200 mV and +500 mV, where oxidation peak of each compound is enhanced; curves in C are details of voltammogram A, in a scanned potential range (E_{app}) comprised between −200 mV and +500 mV, where reduction peak of each compound is enhanced.

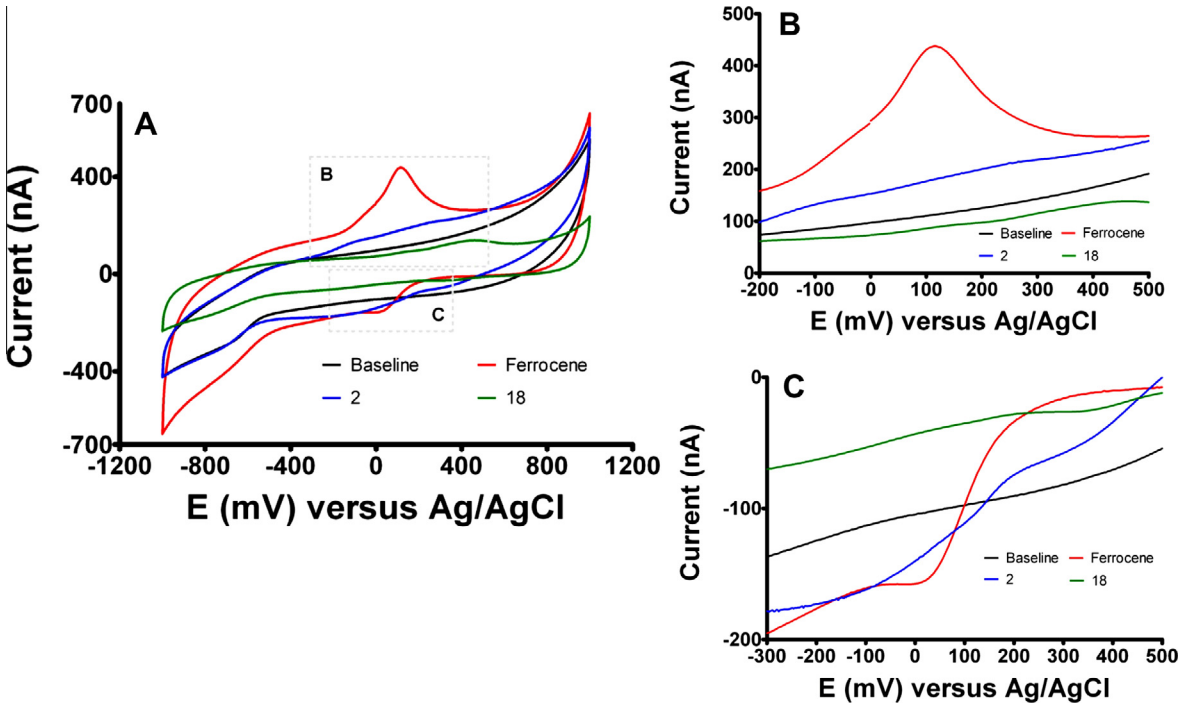

Fig. 5. Cyclic voltammograms recorded with a carbon working electrode (area = 0.071 cm^2), in a buffer solution containing 10 mL of KNO_3 1 M and 10 mL of ethanol 96%. Curves in A, obtained with a scanned potential range (E_{app}) comprised between −1000 mV and +1000 mV, at 100 mV s^{-1} scan rate, were separately achieved, in the absence and in the presence of 1 mM ferrocene, 1 mM compound **2** and 1 mM compound **18**; curves in B are details of voltammogram A, in a scanned potential range (E_{app}) comprised between −200 mV and +500 mV, where oxidation peak of each compound is enhanced; curves in C are details of voltammogram A, in a scanned potential range (E_{app}) comprised between −300 mV and +500 mV, where reduction peak of each compound is enhanced.

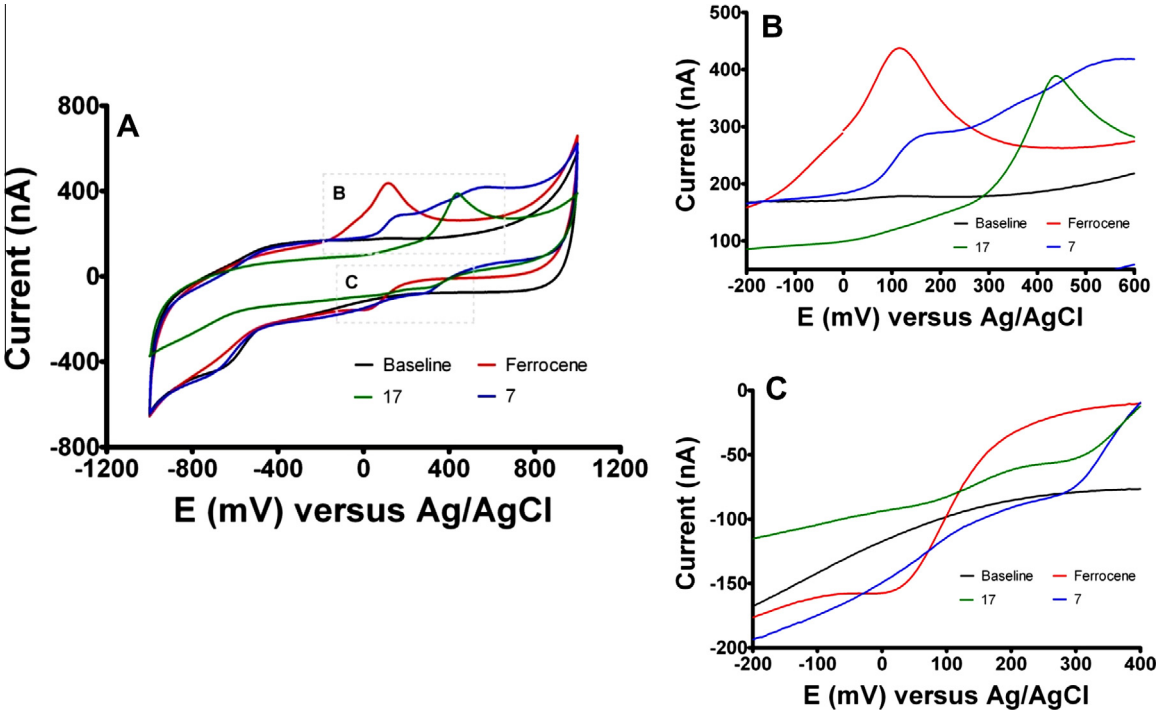

Fig. 6. Cyclic voltammograms recorded with a carbon working electrode (area = 0.071 cm^2), in a buffer solution containing 10 mL of KNO_3 1 M and 10 mL of ethanol 96%. Curves in A, obtained with a scanned potential range (E_{app}) comprised between −1000 mV and +1000 mV, at 100 mV s^{-1} scan rate, were separately achieved, in the absence and in the presence of 1 mM ferrocene, 1 mM compound **7** and 1 mM compound **17**; curves in B are details of voltammogram A, in a scanned potential range (E_{app}) comprised between −200 mV and +600 mV, where oxidation peak of each compound is enhanced; curves in C are details of voltammogram A, in a scanned potential range (E_{app}) comprised between −200 mV and +400 mV, where reduction peak of each compound is enhanced.

Table 1
Electrochemical data for methyl-ketones and ferrocenylchalcones.[a]

	Compound	E_a (mV)	E_c (mV)	ΔE (mV)[b]	status
	Ferrocene	106	36	70	reversible
Monomers	**2**	250	nd	--	not reversible
	18	430	366	64	reversible
	3	nd	nd	--	--
	10	380	320	60	reversible
	6	422	280	142	not reversible
	16	378	306	72	reversible
Dimers	**4**	nd	nd	--	--
	14	400	nd	--	--
	7	150/540	-50/290	200/250	not reversible
	17	430	300	130	not reversible

[a] The analyses were carried out in a buffer solution containing 10 mL of 1 M KNO_3 and 10 mL of 96% ethanol, using a carbon working electrode (area 0.071 mm^2), an Ag/AgCl reference electrode and a Pt counter electrode, with a scanned potential range (V_{app}) comprised between −1000 mV and +1000 mV, at 100 mV s^{-1} scan rate, in the presence of 1 mM of each compound.

[b] $\Delta E = |E_{ox} - E_{red}|$.

radical-scavenging role and the radical-scavenging capacity of iron atom in ferrocene was even higher than that exerted by the phenolic-OH group.

3.3. Biological assay

Several biological studies evidence the use of PC12 cells as straightforward model to evaluate viability and antitumor activity *in vitro* [38–41]. In this work we used PC12 cells to test toxicity of the new ferrocenyl chalcones when used alone and in the presence of hydrogen peroxide (H_2O_2) in order to simulate an oxidative biological process able to promote cell death in cancer cells [42].

Viability of PC12 cells by exposure to compounds **2**–**7**, lacking in ferrocenyl unit, was previously investigated by us [11] and dose–response studies evidenced moderate cytotoxicity at 40 μM only for compounds **3** and **5**, whereas biphenyl **4** significantly induced cell death even at 10 μM concentration.

All ferrocenyl-containing compounds **10**, **14** and **16**–**18** showed a concentration-related toxicity but were less toxic than ferrocene itself on PC12 cells (Fig. 7).

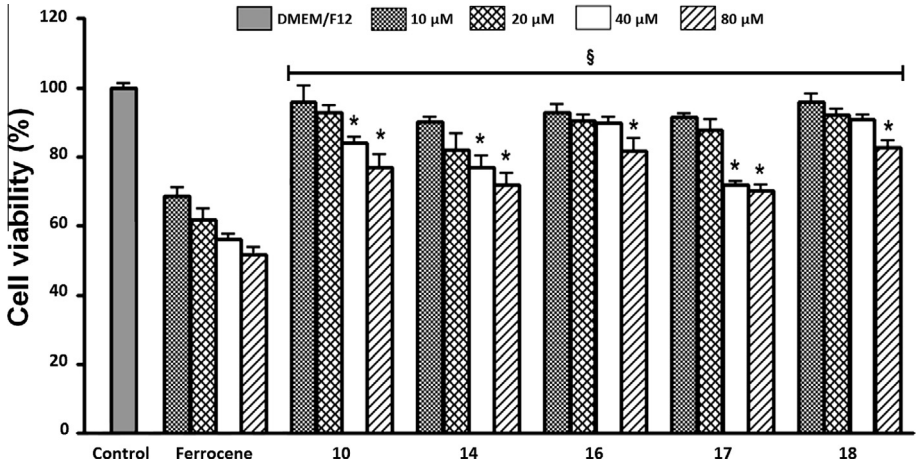

Fig. 7. PC12 cells viability in medium alone (DMEM/F12) or DMEM/F12 plus the compounds ferrocene, **10**, **14**, **16**, **17** and **18** at 10, 20, 40 and 80 μM, respectively. $^{*}P < 0.05$ vs. DMEM/F12 alone (control group). § = $P < 0.05$ vs. ferrocene.

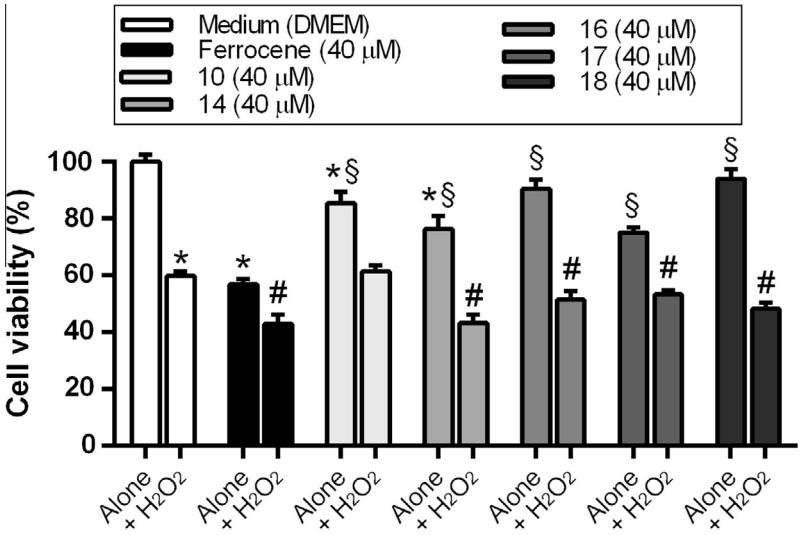

Fig. 8. Viability of PC12 cells in culture medium (DMEM/F12), DMEM/F12 + ferrocene or DMEM/F12 supplemented with H_2O_2 (75 μM), alone and in the presence of compounds **10**, **14**, **16**, **17** and **18** (40 μM). $^{*}P < 0.05$ vs. medium (DMEM/F12) alone. $^{§}P < 0.05$ vs. ferrocene. $^{\#}P < 0.05$ vs. H_2O_2 (75 μM).

At concentration of 40 μM the viability was reduced (about 20%) by exposure to compounds **10**, **14** and **17** whereas roughly doubled decrease was observed in the presence of ferrocene itself comparison with control.

In the series of compounds lacking in the ferrocenyl unit, statistically significant protection from H_2O_2-induced oxidative stress was observed only for dehydrozingerone **2** and zingerone **6** [11].

On the contrary the co-exposure of PC12 to ferrocenyl chalcones **14**, **16**–**18** and H_2O_2, significantly enhanced the cytotoxic effect of hydrogen peroxide resulting in a further decrease of cell viability (see Fig. 8). Although we have not investigated the mechanism of toxicity of the studied ferrocene chalcones in the presence of H_2O_2, generation of hydroxyl anions and highly reactive hydroxyl radicals would occur. In fact, it is generally acknowledged the role of ferrocene unit in producing reactive oxygen species (ROS) in cancer cells due to the innate overproduction of H_2O_2 in these cells [42]. As result of these oxidation reactions, selective oxidative DNA damage of cancer cells and their targeted apoptosis would occur without damage to normal cells. An emerging strategy for cancer treatment exploits the induction of oxidative stress by exogenous ROS generating agents specifically in cancer cells

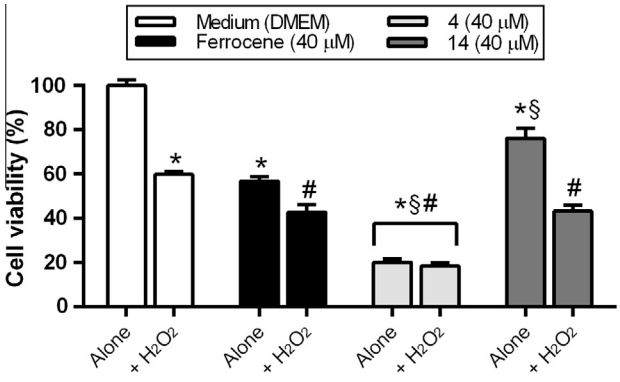

Fig. 9. Viability of PC12 cells in culture medium (DMEM/F12), DMEM/F12 + ferrocene or DMEM/F12 supplemented with H_2O_2 (75 μM), alone and in the presence of compounds **4** and **14** (40 μM). $^{*}P < 0.05$ vs. medium (DMEM/F12) alone. $^{§}P < 0.05$ vs. ferrocene. $^{\#}P < 0.05$ vs. H_2O_2 (75 μM).

leading to their apoptotic death [43] and the antiproliferative activity of some ferrocenyl olefins has been recently related to their ability in inducing ROS generation and cell death [44].

Among the studied ferrocenyl chalcones, the presence of a biphenyl structure and *O*Me-protection of the phenolic –OH groups seems to lead to a significant increase of cytotoxicity (compound **14**) whereas the corresponding monomer (compound **10**) exerts a comparable cytotoxic effect to that of hydrogen peroxide. Nevertheless, it is interesting to note that biphenyl **4**, which manifested antiproliferative and apoptotic activities even at 1 μM [10], was quite toxic on PC12 cells whereas the corresponding ferrocenyl analogue, compound **14**, gave roughly fourfold increased level of cell viability (Fig. 9). Although UV–Vis adsorption spectra showed a shift of biphenyl chalcone **14** toward the longer wavelength region respect to biphenyl **4**, no significant electrochemical differences were detected for biphenyls **4** and **14**. The different viability of **4** and **14** towards PC12 cells would follow separated pathways and it is worthy of further investigation.

4. Conclusions

The first ferrocenyl-dehydrozingerone derivatives in monomer and biphenyl form were prepared by straightforward methods and characterized by spectroscopic and electrochemical analysis. Reversible electrochemical effects, directly related with the presence of a ferrocenyl unit in the molecule, were observed for monomer derivatives but not in biphenyl series. The effect of a ferrocenyl unit on cytotoxic activity in PC12 cells was also evaluated and enhanced cell viability with respect to ferrocene itself was detected for all tested compounds. In comparison with biphenyl **4**, a compound that manifested antiproliferative and apoptotic activities and was quite toxic on PC12 cells, the exposure to the ferrocenyl analogue **14** resulted in roughly fourfold increase in the cell viability. This aspect is worth of future studies and further investigation on different biological targets.

Ferrocenyl chalcones **14** and **16**–**18** significantly increased the oxidative stress generated by hydrogen peroxide, a molecule generally accumulated in cancer cells and, recently, studied as prodrug. Compounds able to activate oxidative stress in cancer cells are promising candidates for a new approach to prodrug activation.

Acknowledgements

This work was supported by Regione Autonoma Sardegna (L.R. 7/2007) which is acknowledged.

Appendix A. Supplementary data

Supplementary data associated with this article can be found, in the online version, at http://dx.doi.org/10.1016/j.poly.2016.05.039.

References

[1] B.B. Aggarwal, G. Sethi, V. Baladandayuthapani, S. Krishnan, S.J. Shishodia, Cell. Biochem. 102 (2007) 580.
[2] Y. Zhou, Y. Zhao, K.M. O'Boyle, P.V. Murphy, Biorg. Med. Chem. Lett. 18 (2008) 954.
[3] T. Esatbeyoglu, P. Huebbe, I.M.A. Ernst, D. Chin, A.E. Wagner, G. Rimbach, Angew. Chem., Int. Ed. Engl. 51 (2012) 5308.
[4] A. Marchiani, C. Rozzo, A. Fadda, G. Delogu, P. Ruzza, Curr. Med. Chem. 21 (2014) 204.
[5] V. Galasso, B. Kovac, A. Modelli, M.F. Ottavini, F. Pichierri, J. Phys. Chem. A 112 (2008) 2331.
[6] W.-F. Chen, S.-L. Deng, B. Zhou, L. Yang, Z.-L. Liu, Free Radical Biol. Med. 40 (2006) 526.
[7] Y.J. Wang, M.H. Pan, A.L. Cheng, L.I. Lin, Y.S. Ho, C.-Y. Hsieh, J.-K. Lin, J. Pharm. Biomed. Anal. 15 (1997) 1867.
[8] W.-H. Lee, C.-Y. Loo, M. Bebawy, F. Luk, R.S. Mason, R. Rohanizadeh, Curr. Neuropharmacol. 11 (2013) 338.
[9] A.G. Hampannavar, R. Karpoormath, M.B. Palkar, M.S. Shaikh, Bioorg. Med. Chem. 24 (2016) 501.
[10] (a) M. Pisano, G. Pagnan, M.A. Dettori, S. Cossu, I. Caffa, I. Sassu, L. Emionite, D. Fabbri, M. Cilli, F. Pastorino, G. Palmieri, G. Delogu, M. Ponzoni, C. Rozzo, Mol. Cancer 9 (2010) 137;
(b) M.A. Dettori, D. Fabbri, M. Pisano, C. Rozzo, G. Palmieri, A. Dessì, R. Dallocchio, G. Delogu, Lett. Drug Des. Discov. 12 (2015) 131.
[11] A. Marchiani, S. Mammi, G. Siligardi, R. Hussain, I. Tessari, L. Bubacco, G. Delogu, D. Fabbri, M.A. Dettori, D. Sanna, S. Dedola, P.A. Serra, P. Ruzza, Amino Acids 45 (2013) 327.
[12] S. Fujisawa, T. Atsumi, Y. Murakami, Y. Kadoma, Arch. Immunol. Ther. Exp. 53 (2005) 28.
[13] V. Kancheva, A. Slavova-Kazakova, D. Fabbri, S. Angelova, M.A. Dettori, J. Nechev, G. Delogu, C. R. Acad. Bulg. Sci. 66 (2013) 361.
[14] P. Messina, E. Labbé, O. Buriez, E.A. Hillard, A. Vessières, D. Hamels, S. Top, G. Jaouen, Y.M. Frapart, D. Mansuy, C. Amatore, Chem. Eur. J. 18 (2012) 6581–6587.
[15] Y.L.K. Tan, P. Pigeon, S. Top, E. Labbé, O. Buriez, E.A. Hillard, A. Vessières, C. Amatore, W.K. Leong, G. Jaouen, Dalton Trans. 41 (2012) 7537.
[16] J.-P. Monserrat, G.G. Chabot, L. Hamon, L. Quentin, D. Scherman, G. Jaouen, E.A. Hillard, Chem. Commun. 46 (2010) 5145.
[17] A. Mooney, A.J. Corry, C. Ruairc, T. Mahgoub, D. O'Sullivan, N. O'Donovan, J. Crown, S. Varughese, S.M. Draper, D.K. Rai, P.T.M. Kenny, Dalton Trans. 39 (2010) 8228.
[18] M.C. Gimeno, H. Goitia, A. Laguna, M.E. Luque, M.D. Villacampa, C. Sepúlveda, M.J. Meireles, Inorg. Biochem. 105 (2011) 1373.
[19] Nabi, Z.Q. Liu, Bioorg. Med. Chem. Lett. 21 (2011) 944–946.
[20] K.N. Tiwari, J.-P. Monserrat, A. Hequet, C. Ganem-Elbaz, T. Cresteil, G. Jaouen, A. Vessières, E.A. Hillard, C. Jolivalt, Dalton Trans. 41 (2012) 6451.
[21] A. Pejović, I. Damljanović, D. Stevanović, M. Vukićević, S.B. Novaković, G.A. Bogdanović, N. Radulović, R.D. Vukićević, Polyhedron 31 (2012) 789.
[22] T. Itoh, S. Shirakami, Y. Nakao, T. Yoshida, Chem. Lett. 27 (1998) 979.
[23] S. Sato, S. Takenaka, Anal. Sci. 28 (2012) 643.
[24] A. Arezki, G.G. Chabot, L. Quentin, D. Scherman, G. Jaouen, E. Brulé, Med. Chem. Commun. 2 (2011) 190.
[25] P.-Z. Li, Z.-Q. Liu, Eur. J. Med. Chem. 46 (2011) 1821.
[26] T.R. Mosmann, J. Immunol. Methods 65 (1983) 55.
[27] M. Iwami, T. Shiina, H. Hirayama, T. Shima, T. Takewaki, Y. Shimizu, J. Nat. Med. 65 (2011) 89.
[28] H. Kabuto, M. Nishizawa, M. Tada, C. Higashio, T. Shishibori, M. Kohno, Neurochem. Res. 30 (2005) 325.
[29] S.-G. Shin, J.Y. Kim, H.Y. Chung, J.-C. Jeong, J. Agric. Food Chem. 63 (2005) 7617–7622.
[30] M.K. Kim, S.W. Chung, D.H. Kim, J.M. Kim, E.K. Lee, J.Y. Kim, Y.M. Ha, Y.H. Kim, J.-K. No, H.S. Chung, K.-Y. Park, S.H. Rhee, J.S. Choi, B.P. Yu, T. Yokozawa, Y.J. Kim, H.Y. Chung, Exp. Gerontol. 45 (2010) 419.
[31] A. Patti, S. Pedotti, T. Grassi, A. Idolo, M. Guido, A. De Donno, J. Organomet. Chem. 716 (2012) 216.
[32] J. Wang, in: J. Wang (Ed.), Analytical Electrochemistry, second ed., Wiley-VCH, New York, 2000. 0-471-28272-3 ISBNs: (Hardback), 0-471-22823-0 (Electronic).
[33] T. Liu, X. Zheng, W. Huang, K. Wu, Colloids Surf. B 65 (2008) 226.
[34] X. Yang, M. Gao, H. Hu, H. Zhang, Phytochem. Anal. 22 (2011) 291.
[35] Z. Ratković, Z.D. Juranić, T. Stanojković, D. Manojlovć, R.D. Vukićević, N. Radulović, M.D. Joksović, Bioorg. Chem. 38 (2010) 26.
[36] J. Maynadié, B. Delavaux-Nicot, S. Fery-Forgues, D. Lavabre, R. Mathieu, Inorg. Chem. 41 (2002) 5002.
[37] B. Delavaux-Nicot, J. Maynadié, D. Lavabre, S. Fery-Forgues, Inorg. Chem. 45 (2006) 5691.
[38] M.A. Siddiqui, M.P. Kashyap, V. Kumar, V.K. Tripathi, V.K. Khanna, S. Yadav, A.B. Pant, Hum. Exp. Toxicol. 30 (2011) 192.
[39] C. Pan, G.S. Giraldo, H. Prentice, J.-Y. Wu, J. Biomed. Sci. 17 (2010) S17.
[40] O. Krizanova, I. Steliarova, L. Csaderova, M. Pastorek, S. Hudecova, Oncol. Rep. 31 (2014) 581.
[41] X. Zang, X. Wang, L. Qin, T. Xu, Z. Zhu, Zhong, S.M. Zhang, Z. Shen, Urology 85 (2015) 273. e 1–7.
[42] W.A. Wlassoff, C.D. Albright, M.S. Sivashinski, A. Ivanova, J.G. Appelbaum, R.I. Salganik, J. Pharm. Pharmacol. 59 (2007) 1549.
[43] B. Kwon, E. Han, W. Yang, W. Cho, W. Yoo, J. Hwang, B.-M. Kwon, D. Lee, ACS Appl. Mater. Interfaces 8 (2016) 5887.
[44] A. Sun, J. Lin, C. Pi, R. Xu, X. Cui, Arch. Pharm. Chem. Life Sci. 349 (2016) 186.